Bloch wave deafness and modal conversion at a phononic crystal boundary

Vincent Laude, Rayisa P. Moiseyenko, Sarah Benchabane, Nico F. Declercq

Bloch wave deafness and modal conversion at a phononic crystal boundary

Vincent Laude, Rayisa P. Moiseyenko, Sarah Benchabane, and Nico F. Declercq

Citation: AIP Advances **1**, 041402 (2011); doi: 10.1063/1.3675828
View online: http://dx.doi.org/10.1063/1.3675828
View Table of Contents: http://aipadvances.aip.org/resource/1/AAIDBI/v1/i4
Published by the American Institute of Physics.

Bloch wave deafness and modal conversion at a phononic crystal boundary

Vincent Laude,[1] Rayisa P. Moiseyenko,[1,2] Sarah Benchabane,[1] and Nico F. Declercq[2]
[1]*Institut FEMTO-ST, Université de Franche-Comté and CNRS, 32 avenue de l'Observatoire, F-25044 Besançon Cedex, France*
[2]*Georgia Institute of Technology, UMI Georgia Tech – CNRS, George W. Woodruff School of Mechanical Engineering, Georgia Tech Lorraine, 2 rue Marconi, 57070 Metz-Technopole, France*

(Received 31 October 2011; accepted 9 December 2011; published online 23 December 2011)

We investigate modal conversion at the boundary between a homogeneous incident medium and a phononic crystal, with consideration of the impact of symmetry on the excitation of Bloch waves. We give a quantitative criterion for the appearance of deaf Bloch waves, which are antisymmetric with respect to a symmetry axis of the phononic crystal, in the frame of generalized Fresnel formulas for reflection and transmission at the phononic crystal boundary. This criterion is used to index Bloch waves in the complex band structure of the phononic crystal, for directions of incidence along a symmetry axis. We argue that within deaf frequency ranges transmission is multi-exponential, as it is within frequency band gaps. [doi:10.1063/1.3675828]

I. INTRODUCTION

As periodic composite media, phononic crystals (PC) support elastic or acoustic waves whose properties are prescribed through the Bloch-Floquet theorem.[1,2] The eigenmodes of the Helmholtz equation for monochromatic wave propagation are called Bloch waves and are each associated with a $(\omega, \mathbf{k})$ pair, with ω the angular frequency and $\mathbf{k}$ the Bloch wavevector. For propagating Bloch waves, the wavevector can be folded inside the first Brillouin zone, whereas for evanescent Bloch waves this rule applies only to the real part of the wavevector.[3–5] Experimental investigations of the dispersion of a PC usually rely on the excitation of Bloch waves by an external source, for instance by monitoring the transmission of a particular mode of the medium surrounding a finite size PC.[6–8] It is thus clear that the intrinsic properties of the PC are only explored through modal conversions that occur at the boundary between the surrounding medium and the PC. Obviously, modal conversion to different Bloch waves results in different conversion efficiencies. A particularly striking example is the experimental observation of the non excitation of certain Bloch waves, that have thus been termed deaf.[9]

Deaf Bloch waves were originally observed in two-dimensional (2D) PC of rigid rods in air arranged according to a square lattice.[9–12] They were soon to be also found in three-dimensional (3D) PC of solid spheres in a solid[13,14] or a fluid matrix,[15] and in 2D PC of steel rods in water with hexagonal-type lattices.[16] Recently, they have also been observed in phononic crystal slabs.[17–19] Deaf Bloch waves manifest themselves as dips in the transmission, much as band gaps do, and thus lead to discrepancies between the theoretical band structure and the experimental result. This discrepancy is soon explained by observing that a plane wave incident normally on the PC is symmetric with respect to the propagation direction; if a particular Bloch wave is antisymmetric with respect to the same axis, then it cannot be excited and it cannot contribute to transmission through the PC. In the band structure, bands formed by deaf Bloch waves are by extension termed deaf bands.

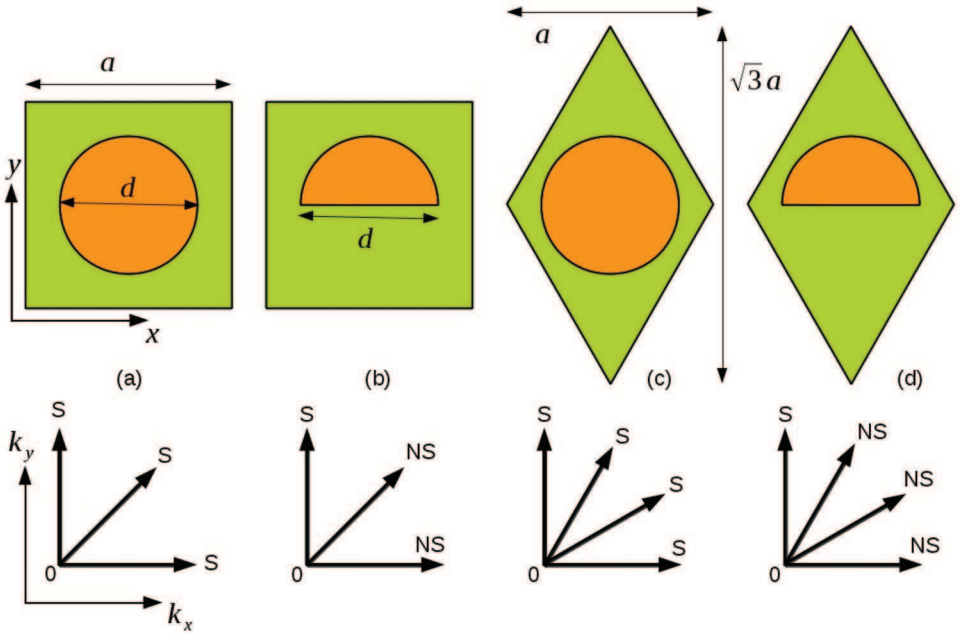

FIG. 1. Unit-cells for square and hexagonal lattice 2D phononic crystals, containing either a circular or a semi-circular inclusion. Regarding wave propagation, the circular inclusion preserves all symmetry directions of the lattice, while the semi-circular inclusion only preserves symmetry along the y axis. Symmetric (S) and non symmetric (NS) directions are shown for each case.

In this paper, we examine modal conversion at the boundary between a homogeneous incident medium and a phononic crystal, with consideration of the impact of symmetry on the excitation of Bloch waves. Consideration of symmetry is indeed essential for modal conversion and the appearance of deaf Bloch waves, as is illustrated in Section II. We specifically discuss the curing of deafness by breaking the symmetry of the unit-cell of the PC. In Section III, we consider the problem of modal conversion to a Bloch wave from an external medium and obtain a numerical criterion for deciding if a Bloch wave is deaf or not. We find that evanescent Bloch waves and their symmetries must explicitly be taken into account. Then in Section IV we derive generalized Fresnel formulas that relate the amplitudes of reflected and transmitted waves to the amplitudes of incident waves. From these formulas, we explicitly show that deaf Bloch waves cannot be excited by a symmetric incident plane wave. Finally, in Section V the symmetry of Bloch waves is related to their internal order of diffraction and used to index complex band structures. This procedure permits the separation of band foldings occurring at symmetry points of the Brillouin zone from bands becoming propagating above a given cut-off frequency.

II. DEAFNESS AND UNIT-CELL SYMMETRY

Let us consider 2D phononic crystals such as depicted in Figure 1. Two different lattices are shown, square (SQ) and hexagonal (HEX). The SQ lattice has symmetries with respect to axes x and y and with respect to both diagonals, i.e., every $n\pi/4$ with n an integer. The HEX lattice has symmetries every $n\pi/6$. Two different inclusions are further considered, either a circle or a semi-circle. While the circular inclusion preserves all lattice symmetries, the semi-circular inclusion only preserves symmetry along the y axis. It is thus the combination of the symmetries of lattice and inclusions that defines the symmetry of the unit-cell of the PC. Of course, an inclusion of arbitrary shape generally removes any symmetry.

Let us now consider wave propagation in the PC. For the sake of simplicity, we consider in this paper only the case of pressure waves in water. In the following numerical examples, inclusions are composed of steel and only longitudinal waves are considered. This approximation neglects

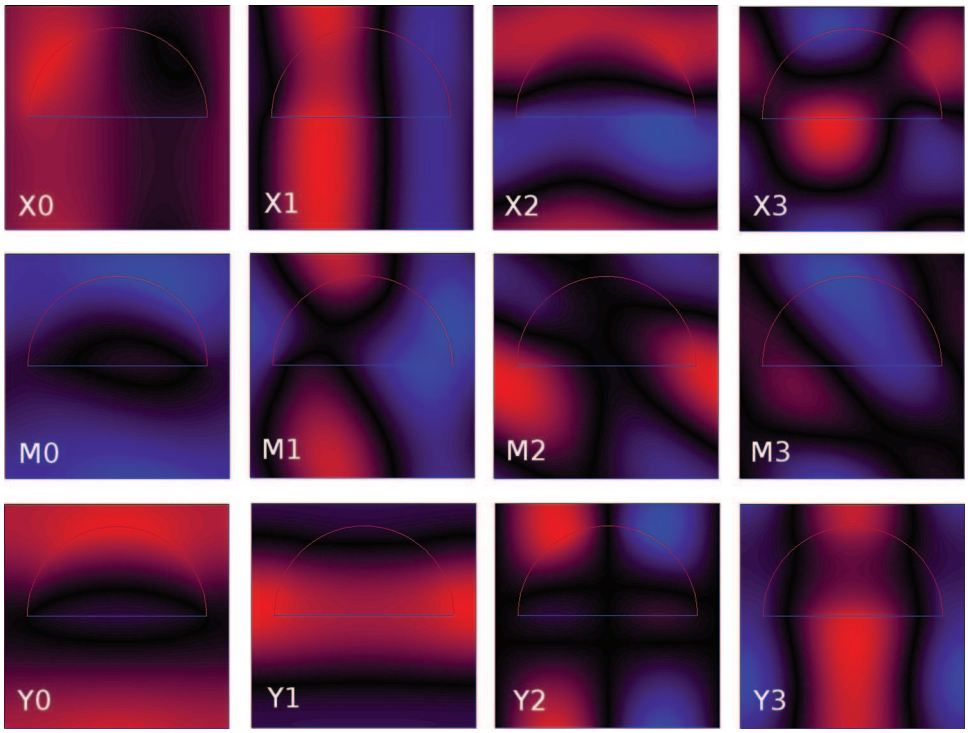

FIG. 2. Pressure fields of Bloch waves depicted for a square-lattice phononic crystal of steel half-cylinders in water with $d/a = 0.8$ (unit-cell shown in Fig. 1(b)). First line: first 4 Bloch waves for $\kappa_x = 0.4$ and $\kappa_y = 0$ (X direction of the first Brillouin zone). Second line: first 4 Bloch waves for $\kappa_x = 0.4$ and $\kappa_y = 0.4$ (M direction of the first BLZ). Third line: first 4 Bloch waves for $\kappa_x = 0$ and $\kappa_y = 0.4$ (Y direction of the first BLZ).

shear waves in the steel inclusions but has been found to give results comparable with more exact fluid-solid computations. The Bloch-Floquet theorem states that for a fixed angular frequency ω, the modes of the phononic crystal have the form

$$p(\mathbf{r}, t) = \bar{p}(\mathbf{r}) \exp(\imath(\omega t - \mathbf{k} \cdot \mathbf{r})) \tag{1}$$

where $\mathbf{k}$ is the Bloch wavevector and $\bar{p}(\mathbf{r})$ is a periodic function in the unit-cell. For convenience, we consider in the following reduced wavevectors defined as $\boldsymbol{\kappa} = \mathbf{k}a/(2\pi)$. The symmetry directions of the PC are shared by Bloch waves. It can further be inferred that if the unit-cell has a symmetry direction, then Bloch waves having their wavevector pointing in that direction part into two groups, symmetric and antisymmetric.

As an example, we consider in Fig. 2 some Bloch waves of a square-lattice PC with semi-circular inclusions, as depicted in Fig. 1(b). Three directions of propagation are considered: along x (direction X), along y (direction Y), and along the first diagonal (direction M). The first 4 Bloch waves are plotted in each case. It can be seen that for direction Y, Bloch waves number 0, 1 and 3 are symmetric, while Bloch wave number 2 is antisymmetric. The latter is an example of a deaf Bloch wave. In contrast, there are no special symmetries for the Bloch waves of directions X and M. If the inclusion had been circular, Bloch waves in direction X would have been identical to those in direction Y, and Bloch waves number 1 and 3 would have been antisymmetric and thus deaf. Even in the case of a symmetric lattice and a symmetric inclusion, there is a simple way to break symmetry: it is sufficient to consider a wavevector that is not along a direction of symmetry. As a result, changing the angle of incidence even slightly generally removes deafness from all Bloch waves.

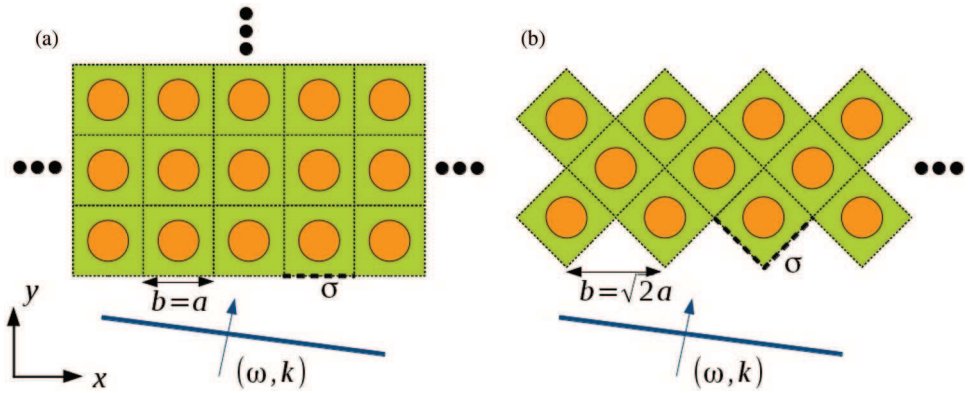

FIG. 3. Modal conversion problem for a plane wave incident on the boundary of a phononic crystal. The two cases shown are for a square-lattice 2D PC cut either along (a) direction X and (b) direction M.

III. A CRITERION FOR DEAFNESS

Bloch waves discussed in the previous section are intrinsic modes of the PC. In practice, the PC is of finite extent and has boundaries separating it from the surrounding medium. Fig. 3 depicts such a boundary for a square-lattice PC. Two cases have been illustrated, with the PC cut along symmetry direction X or M. It can be noted that the periodicity along the PC boundary, b, is different in both cases. A plane wave with angular frequency ω and wavevector $\mathbf{k}_0$ is incident on the PC boundary. The incident pressure field is

$$p_i(\mathbf{r}, t) = \exp(\imath(\omega t - k_{0x}x - k_{0y}y)), \tag{2}$$

with the dispersion relation $k_{0x}^2 + k_{0y}^2 = \omega^2/c^2$ and c the velocity in the incident medium. There is a certain degree of arbitrariness in the exact choice of boundary σ; in Fig. 3 we have chosen it to lie exactly on the boundary of the unit-cell, but other choices can be made without changing the result of the analysis conducted in this section.

We next examine the conversion of the incident wave to Bloch waves. Conservation of energy and momentum requests conservation of the frequency and of the x component of the wavevector. Thus, the relevant Bloch waves in the PC are given as solutions of a problem of the form $k_y(\omega; k_{0x})$ that yields a discrete set of complex-valued solutions k_{ny}, with n the mode index.[3] Anticipating the results of the next Section, we consider the scalar product between the incident wave and the n-th Bloch wave, measured along the PC boundary σ, as a measure of modal conversion. This quantity reduces to a line integral of the periodic part of the Bloch wave solution

$$\langle p_i(\omega; k_{0x}) | p_n(\omega; k_{0x}) \rangle = \int_\sigma ds \exp(\imath(k_{0y} - k_{ny})y) \bar{p}_n(\mathbf{r}). \tag{3}$$

In the particular case that σ is a simple straight line, as in Fig. 3(a), we can take the integral along $y = 0$, in which case the above equation reduces to

$$\langle p_i(\omega; k_{0x}) | p_n(\omega; k_{0x}) \rangle = \int_\sigma ds \bar{p}_n(\mathbf{r}). \tag{4}$$

Even though the incident wavevector doesn't appear explicitly in this expression, both k_{ny} and $\bar{p}_n(\mathbf{r})$ depend on the pair $(\omega; k_{0x})$.

Equation (4) contains all the observations and results of the previous section. Obviously, if the periodic part of the Bloch wave, $\bar{p}_n(\mathbf{r})$, is antisymmetric, then the scalar product is zero. For normal incidence, i.e. $k_{0x} = 0$, this property remains true whatever the value of k_{ny} and deaf Bloch waves form deaf bands. When incidence is not normal, i.e. $k_{0x} \neq 0$, deafness is lost immediately since the wavevector breaks the symmetry. We have indeed verified numerically that deafness is highly sensitive to the incidence angle: the scalar product in Eq. (4) deviates from zero as soon as $k_x \neq 0$.

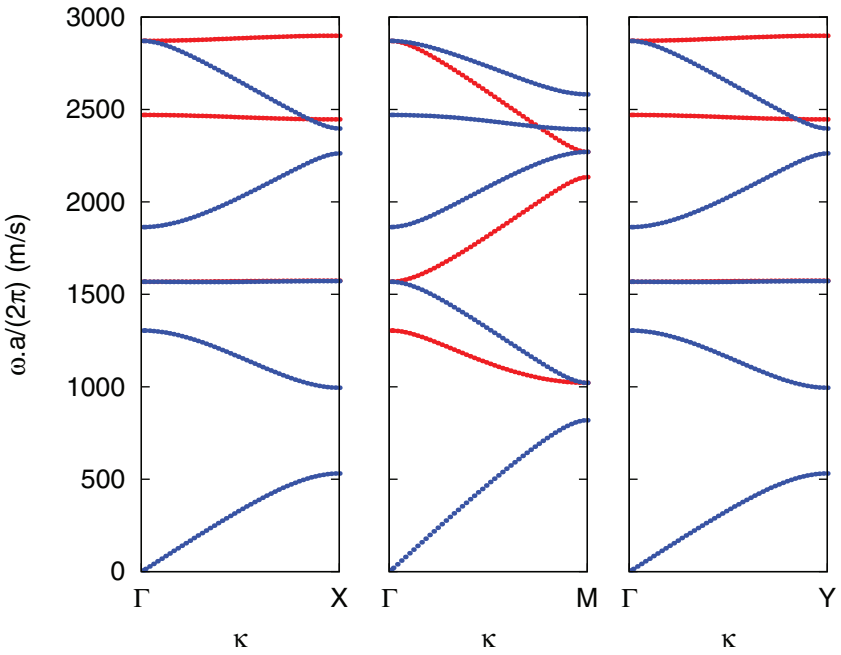

FIG. 4. Band structure for a square-lattice 2D PC of circular steels rods in water with $d/a = 0.8$, shown along direction X, M and Y in the first Brillouin zone. Antisymmetric (deaf) bands appear in red, while symmetric (non deaf) bands appear in blue. Note that bands 3 and 4 in directions X and Y are degenerate in frequency, but that band 3 is deaf while band 4 is not.

The line integral defined above provides a simple means of evaluating the symmetry or antisymmetry of Bloch waves for normal incidence. It can thus be used to investigate the intrinsic symmetry properties of band structures. Fig. 4 and Fig. 5 display band structures for propagating Bloch waves for a square-lattice 2D PC of steels rods in water, in the case of the circular and of the semi-circular inclusion depicted in Fig. 1(a) and Fig. 1(b), respectively. These band structures are obtained as a solution of the $\omega(\mathbf{k})$ eigenvalue problem for $\mathbf{k}$ varying along particular directions of the first Brillouin zone. Bands holding deaf Bloch waves are plotted in red, while bands holding non deaf Bloch waves are plotted in blue. For the circular inclusion, Fig. 4, the three symmetry directions X, M, and Y show deaf bands, and directions X and Y are equivalent. For the semi-circular inclusions that only preserve symmetry along direction Y, deaf bands only appear along this same direction, as Fig. 5 illustrates. It can further be observed that the complete band gap observed in the case of a circular inclusion disappears for the semi-circular inclusion.

IV. GENERALIZED FRESNEL FORMULAS

We discuss in this Section how the problem of modal conversion at the PC boundary can be cast in the form of generalized Fresnel formulas. The PC boundary has a periodic corrugation and thus acts as a diffraction grating with period b. Reflected diffraction orders have the form of plane waves satisfying the grating law. The m-th reflected diffraction order is the plane wave

$$p_{mr}(\mathbf{r}, t) = \exp(\imath(\omega t - k_{mx}x - k_{my}y)), \tag{5}$$

with $k_{mx} = k_{ox} + 2\pi m/b$, and $k_{my} = -\sqrt{\omega^2/c^2 - k_{mx}^2}$ or $k_{my} = \imath\sqrt{|\omega^2/c^2 - k_{mx}^2|}$ for propagating and evanescent reflected waves, respectively. Reflected diffraction orders can be cast in the Bloch-Floquet form by observing that $\mathbf{k}_m = (k_{0x}, k_{my})$ and $\bar{p}_{mr}(\mathbf{r}) = \exp(-\imath 2\pi m x/b)$. Note that incident diffraction orders assume exactly the same form but with the reverse sign in the definition of k_{my}.

Continuity equations for pressure and normal velocity are next expressed along boundary σ. For simplicity, we consider in the following that σ is along $y = 0$, but the general case is not significantly

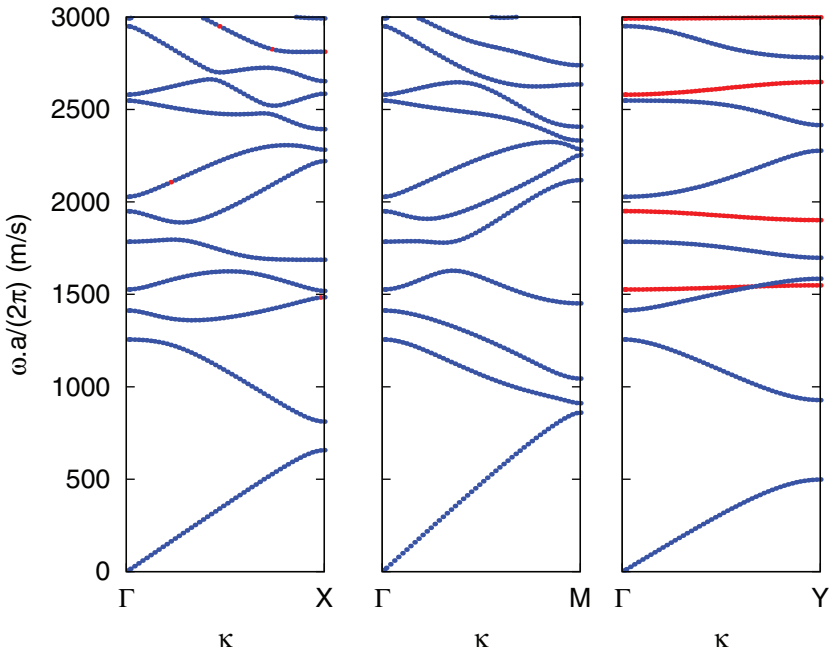

FIG. 5. Band structure for a square-lattice 2D PC of semi-circular steels rods in water with $d/a = 0.8$, shown along direction X, M and Y in the first Brillouin zone. Antisymmetric (deaf) bands appear in red, while symmetric (non deaf) bands appear in blue.

different. The continuity equations have the form

$$v_i(\mathbf{r}, t) + \sum_m r_m v_{mr}(\mathbf{r}, t) = \sum_n t_n v_n(\mathbf{r}, t), \tag{6}$$

$$p_i(\mathbf{r}, t) + \sum_m r_m p_{mr}(\mathbf{r}, t) = \sum_n t_n p_n(\mathbf{r}, t), \tag{7}$$

where the r_m are the reflected amplitudes and the t_n are the transmitted amplitudes. p_n and v_n are the pressure and the normal velocity distributions of the n-th Bloch wave, respectively. The expansion over Bloch waves implicitly assumes that these functions constitute a complete basis for the solution of the Helmholtz equation in the PC.[3] Reflected diffraction orders satisfy[20]

$$v_{mr} = \frac{k_{my}}{\rho\omega} p_{mr} = \frac{-1}{Z_m} p_{mr}, \tag{8}$$

where Z_m is the mechanical impedance of the m-th diffraction order. The minus sign in the definition of the impedance Z_m accounts for reflection. Incident diffraction orders similarly satisfy $v_{mi} = \frac{1}{Z_m} p_{mi}$. We next multiply by $\exp(\imath k_{ox} x)\exp(\imath 2\pi m x/b)$ and integrate along σ. Because of the orthogonality of Fourier exponentials we end up with the matrix relations

$$\frac{1}{Z_m} i_m - \frac{1}{Z_m} r_m = M_v(m, n) t_n \tag{9}$$

$$i_m + r_m = M_p(m, n) t_n \tag{10}$$

with the incident amplitudes $i_m = 1$ if $m = 0$ and $i_m = 0$ otherwise. The matrices

$$M_v(m, n) = \frac{1}{b} \int_\sigma dx \exp(\imath 2\pi m x/b) \bar{v}_n(\mathbf{r}) \tag{11}$$

and

$$M_p(m, n) = \frac{1}{b} \int_\sigma dx \exp(\imath 2\pi m x/b) \bar{p}_n(\mathbf{r}) \tag{12}$$

govern the modal conversion process. Note that the integral in Eq. (4) is proportional to $M_p(0, n)$. Solving the matrix equations (9) and (10) is straightforward and results in a generalized version of the Fresnel formulas for refraction and reflection

$$\mathbf{t} = 2(M_p + ZM_v)^{-1}\mathbf{i} \tag{13}$$

$$\mathbf{r} = (M_p - ZM_v)(M_p + ZM_v)^{-1}\mathbf{i} \tag{14}$$

with the diagonal matrix $Z(m, n) = Z_m\delta(m - n)$. In the above equations, vectors $\mathbf{i}$, $\mathbf{r}$ and $\mathbf{t}$ gather the amplitudes of the incident, reflected and transmitted waves, respectively.

The traditional Fresnel formulas[20] must obviously be recovered when the phononic crystal is replaced by a homogeneous medium. In this case, there is only one reflected and one transmitted wave, and the matrices above simplify to scalars. Let us consider medium A as the incidence medium and medium B as the transmission medium. We have $Z_0^{-1} = Z_A^{-1}\cos\theta_A$, with $Z_A = \rho_A c_A$ and θ_A the angle of incidence. For the transmitted wave, $M_v/M_p = Z_B^{-1}\cos\theta_B$ or $-\imath|k_y|/(\rho_B\omega)$ if it is propagating or evanescent, respectively. It follows that $r = \frac{Z_B\cos\theta_A - Z_A\cos\theta_B}{Z_B\cos\theta_A + Z_A\cos\theta_B}$ if the transmitted wave is propagating and $|r| = 1$ if it is evanescent.

We next show that anti-symmetric Bloch waves are not excited in the case of normal incidence on a PC that is symmetric with respect to the direction of incidence. To that end, we first rearrange the order of Bloch waves of the PC so has to separate symmetric (S) and antisymmetric (AS) Bloch waves

$$\mathbf{t} = \begin{pmatrix} \mathbf{t}_S \\ \mathbf{t}_{AS} \end{pmatrix} \tag{15}$$

Because of normal incidence, we can also recast the reflected diffraction orders into Bloch waves in the incident medium with $\mathbf{k}_m = (k_{0x}, k_{my})$, with $\bar{p}_{mr}(\mathbf{r}) = \cos(2\pi mx/b)$ for $m \geq 0$ (S) or $\sin(2\pi mx/b)$ for $m > 0$ (AS). To achieve this reordering, it is sufficient to recombine the original diffraction orders m and $-m$. Matrices M_p and M_v then become block-diagonal, e.g.,

$$M_p = \begin{pmatrix} M_{p,\mathrm{S}} & 0 \\ 0 & M_{p,\mathrm{AS}} \end{pmatrix}, \tag{16}$$

Since the incident plane wave is itself symmetric, we conclude that $\mathbf{t}_{AS} = 0$ and $\mathbf{r}_{AS} = 0$, i.e., antisymmetric (deaf) Bloch waves are not transmitted and antisymmetric reflected diffraction orders are not excited. This is a demonstration of the properties that were introduced in the previous sections based on intuition.

V. COLORING COMPLEX BAND STRUCTURES

We plotted in Fig. 4 and Fig. 5 band structures with the information of symmetry (non deafness) or antisymmetry (deafness). Though the added information is useful to compare with experiments, it does not bring clear physical insight on the formation of band gaps or on the origin of the various bands. Nevertheless, it is clear that symmetry properties apply to Bloch waves irrespective of their propagating or evanescent character. We then display in Fig. 6 and Fig. 7 complex band structures with symmetry information for all types of Bloch waves. Fig. 6 can be compared directly with Fig. 4, and Fig. 7 with Fig. 5.

In direction M and for the circular inclusion, systems of band gaps for S and AS Bloch waves are observed in the complex band structure of Fig. 6. This is expected, since S and AS Bloch waves are decoupled, but it would have been difficult to distinguish them without information about symmetry. The first frequency band gap appears when the fundamental S Bloch wave reaches the M point of the first Brillouin zone, for $\omega a/(2\pi)$ ranging between 800 and 1000 m/s, approximately. Within this frequency range, there are only evanescent Bloch waves. It is then expected that transmission is multi-exponential,[21] with only S evanescent Bloch waves contributing to transmission for a symmetric source. The dominant S Bloch wave in the transmission is the one with the smallest imaginary part of the k-vector. We next point out that the first AS Bloch wave, labeled 1 in Fig. 6, is evanescent at

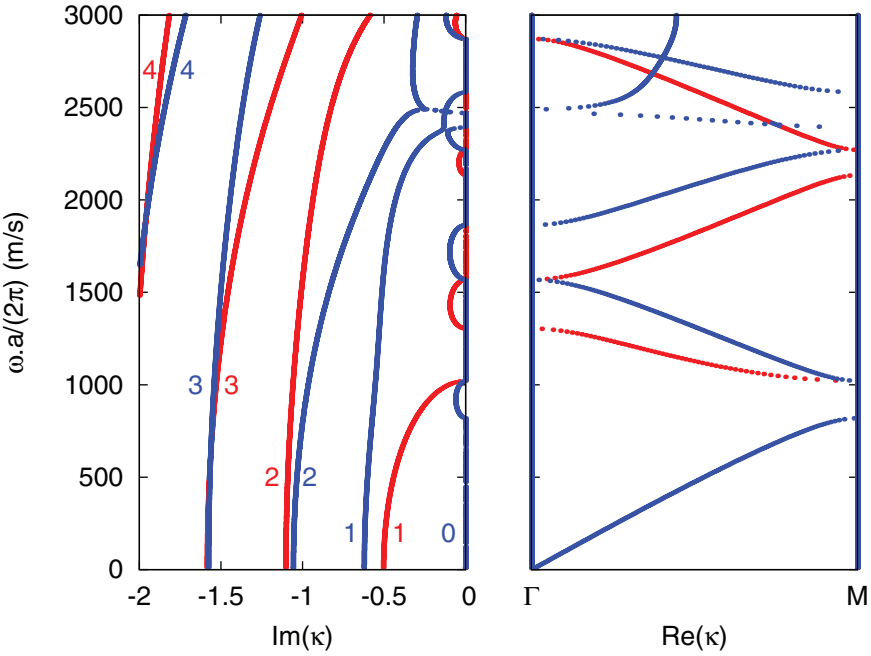

FIG. 6. Complex band structure for a square-lattice 2D PC of circular steels rods in water with $d/a = 0.8$, shown along direction M of the first Brillouin zone. Antisymmetric (deaf) bands appear in red, while symmetric (non deaf) bands appear in blue.

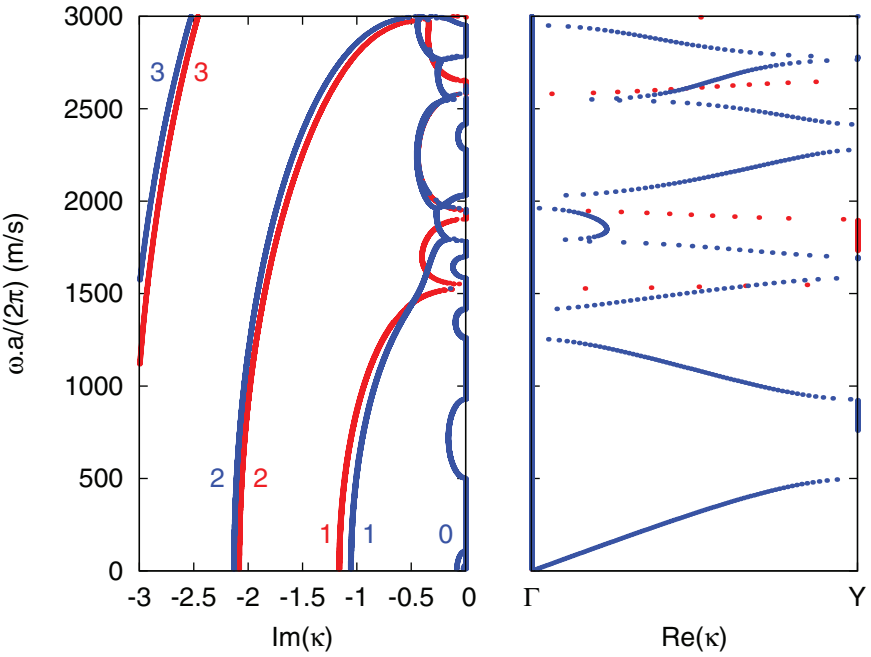

FIG. 7. Complex band structure for a square-lattice 2D PC of semi-circular steels rods in water with $d/a = 0.8$, shown along direction Y of the first Brillouin zone. Antisymmetric (deaf) bands appear in red, while symmetric (non deaf) bands appear in blue.

low frequencies with the real part of the wavevector staying at point M of the first Brillouin zone, and acquires a negative group velocity above its first cut-off frequency. Above its first band gap, for $\omega a/(2\pi)$ above 1550 m/s, all S Bloch waves are evanescent; transmission for a symmetric source is again multi-exponential and governed by the S Bloch wave with the smallest imaginary part of the wavevectors. In direction Y and for the semi-circular inclusion, Fig. 7, the systems of band gaps for S and AS Bloch waves are decoupled again. The rather flat AS bands that were observed in Fig. 5 are seen to be connected by evanescent bands.

VI. CONCLUSION

We have investigated modal conversion at the boundary between a homogeneous incident medium and a phononic crystal. We have emphasized the importance of symmetry on the excitation of Bloch waves. Bloch waves separate between symmetric and antisymmetric provided the wavevector varies along a symmetry axis of the phononic crystal. Generalized Fresnel formulas for reflection and transmission at the phononic crystal boundary have been obtained and used to show that antisymmetric Bloch waves are not excited by a symmetric incident plane wave and are thus deaf. Symmetry has been further used to index Bloch waves in the complex band structure of the phononic crystal, for directions of incidence along a symmetry axis. It is found in particular that transmission is multi-exponential within deaf frequency ranges, as it is within frequency band gaps.

ACKNOWLEDGMENTS

Financial support by the Agence Nationale de la Recherche under grant ANR-09-BLAN-0167-01 is gratefully acknowledged.

APPENDIX

In this appendix, we summarize the variational formulations that are used in this paper for obtaining band structures and complex band structures based on a finite element method (FEM). The presentation is restricted to the fluid case with longitudinal waves only, but it can be generalized to elastic wave propagation in solids along similar lines. Only modal computations are considered, so there are no applied external forces. The basic equations for propagation of acoustic waves in a fluid are taken as:

$$-\nabla p(\mathbf{r},t) = \rho(\mathbf{r})\frac{\partial \mathbf{v}(\mathbf{r},t)}{\partial t}, \tag{A1}$$

$$\frac{\partial p(\mathbf{r},t)}{\partial t} = -B(\mathbf{r})\nabla\cdot\mathbf{v}(\mathbf{r},t), \tag{A2}$$

where variable dependence have been stressed and will not be repeated in the following. In the computations presented in this paper, we have used $\rho = 1000$ kg/m^3 and $B = 2.2$ GPa for water, and $\rho = 7800$ kg/m^3 and $B = 160$ GPa for steel. Further assuming monochromaticity, we have

$$-\frac{1}{\rho}\nabla p = \imath\omega\mathbf{v}, \tag{A3}$$

$$\omega^2\frac{1}{B}p = \imath\omega\nabla\cdot\mathbf{v} = -\nabla\cdot\left(\frac{1}{\rho}\nabla p\right). \tag{A4}$$

From the Bloch-Floquet theorem as expressed by Eq. (1), the unknown fields are $\bar{p}$ and $\bar{\mathbf{v}}$, and each solution is associated with a pair $(\omega, \mathbf{k})$. Space differentiation follows the rule

$$\nabla p = (\nabla\bar{p} - \imath\mathbf{k}\bar{p})\exp(\imath(\omega t - \mathbf{kr})) \tag{A5}$$

Multiplying with a test function $\bar{q}$, integrating over the domain, and performing an integration by parts, we obtain

$$\omega^2 \int_\Omega d\mathbf{r} \left(\bar{q}^* \frac{1}{B} \bar{p} \right) = \int_\Omega d\mathbf{r} \left((\nabla \bar{q} - \imath \mathbf{k} \bar{q})^\dagger \frac{1}{\rho} (\nabla \bar{p} - \imath \mathbf{k} \bar{p}) \right), \forall q \tag{A6}$$

This variational equation is used to obtain band structures by varying the wavevector in the first Brillouin zone. As a result of Hermitian symmetry in case the material parameters are purely real (no material loss), the resulting eigenvalue problem for ω^2 has only real and positive solutions. The FEM formulation only requires truly periodic boundary conditions. Hussein[22] proposes a similar approach for elastic waves in solids.

To obtain a variational formulation of the complex band structure of a phononic crystal, we seek to obtain an eigenvalue equation for the modulus of $\mathbf{k}$ while ω is a now a parameter. We write[3]

$$\mathbf{k} = k\boldsymbol{\alpha} + \mathbf{k}_0 \tag{A7}$$

where $\boldsymbol{\alpha}$ is a unit vector accounting for a direction in reciprocal (Brillouin) space and $\mathbf{k}_0$ is a fixed point in the same space. In the following, $\nabla \bar{p}$ must be understood as a shorthand for $\nabla \bar{p} - \imath \mathbf{k}_0 \bar{p}$. We rewrite Equations (A3) and (A4)

$$-\frac{1}{\rho} \nabla \bar{p} + \imath k \boldsymbol{\alpha} \frac{1}{\rho} \bar{p} = \imath \omega \bar{\mathbf{v}} \tag{A8}$$

$$\omega^2 \frac{1}{B} \bar{p} = \nabla \cdot (\imath \omega \bar{\mathbf{v}}) - \imath k \boldsymbol{\alpha} \cdot (\imath \omega \bar{\mathbf{v}}). \tag{A9}$$

Next we define the normal acceleration (or acceleration along the propagation direction) as

$$\phi = \imath \omega \boldsymbol{\alpha} \cdot \bar{\mathbf{v}} \tag{A10}$$

and we transform the two equations above to the two scalar equations

$$-\boldsymbol{\alpha} \cdot \frac{1}{\rho} \nabla \bar{p} + \imath k \frac{1}{\rho} \bar{p} = \phi \tag{A11}$$

$$\omega^2 \frac{1}{B} \bar{p} = -\nabla \cdot (\frac{1}{\rho} \nabla \bar{p}) + \imath k (\nabla \cdot \boldsymbol{\alpha}) \frac{1}{\rho} \bar{p} - \imath k \phi. \tag{A12}$$

Rearranging the terms we get

$$\phi + \frac{1}{\rho} (\boldsymbol{\alpha} \cdot \nabla) \bar{p} = \imath k \frac{1}{\rho} \bar{p} \tag{A13}$$

$$\omega^2 \frac{1}{B} \bar{p} + \nabla \cdot (\frac{1}{\rho} \nabla \bar{p}) = \imath k (\boldsymbol{\alpha} \cdot \nabla) \frac{1}{\rho} \bar{p} - \imath k \phi. \tag{A14}$$

A variational form of these equations is obtained by considering a vector of two test functions $(\psi, \bar{q})$ living in the same finite element space as $(\phi, \bar{p})$

$$\int_\Omega d\mathbf{r} A(\psi, \bar{q}; \phi, \bar{p}) = (\imath k) \int_\Omega d\mathbf{r} B(\psi, \bar{q}; \phi, \bar{p}), \forall (\psi, q) \tag{A15}$$

with

$$A(\psi, \bar{q}; \phi, \bar{p}) = \psi^* \phi + \psi^* \frac{1}{\rho} (\boldsymbol{\alpha} \cdot \nabla) \bar{p} + \omega^2 \bar{q}^* \frac{1}{B} \bar{p} - (\nabla \bar{q})^\dagger \frac{1}{\rho} \nabla \bar{p} \tag{A16}$$

$$B(\psi, \bar{q}; \phi, \bar{p}) = \psi^* \frac{1}{\rho} \bar{p} - (\boldsymbol{\alpha} \cdot \nabla \bar{q})^* \frac{1}{\rho} \bar{p} - \bar{q}^* \phi \tag{A17}$$

The matrix form of this variational problem obtained by a FEM again assumes the form of a generalized eigenvalue problem (but now for $\imath k$), with non symmetrical matrices. As a consequence,

the eigenvalues are in general complex. In case B and ρ are real-valued functions, eigenvalues come out as complex conjugate pairs.

[1] M. M. Sigalas and E. N. Economou, "Band structure of elastic waves in two dimensional systems," Solid State Commun. **86**, 141–143 (1993).
[2] M. S. Kushwaha, P. Halevi, L. Dobrzynski, and B. Djafari-Rouhani, "Acoustic band structure of periodic elastic composites," Phys. Rev. Lett. **71**, 2022–2025 (1993).
[3] V. Laude, Y. Achaoui, S. Benchabane, and A. Khelif, "Evanescent Bloch waves and the complex band structure of phononic crystals," Phys. Rev. B **80**, 092301 (2009).
[4] V. Romero-García, J. V. Sánchez-Pérez, S. Castiñeira-Ibáñez, and L. M. Garcia-Raffi, "Evidences of evanescent bloch waves in phononic crystals," Appl. Phys. Lett. **96**, 124102 (2010).
[5] R. P. Moiseyenko and V. Laude, "Material loss influence on the complex band structure and group velocity in phononic crystals," Phys. Rev. B **83**, 064301 (2011).
[6] F. R. Montero de Espinosa, E. Jiménez, and M. Torres, "Ultrasonic band gap in a periodic two-dimensional composite," Phys. Rev. Lett. **80**, 1208–1211 (1998).
[7] A. Khelif, A. Choujaa, B. Djafari-Rouhani, M. Wilm, S. Ballandras, and V. Laude, "Trapping and guiding of acoustic waves by defect modes in a full-band-gap ultrasonic crystal," Phys. Rev. B **68**, 214301 (2003).
[8] A. Khelif, A. Choujaa, S. Benchabane, B. Djafari-Rouhani, and V. Laude, "Guiding and bending of acoustic waves in highly confined phononic crystal waveguides," Appl. Phys. Lett. **84**, 4400–4002 (2004).
[9] J. V. Sánchez-Pérez, D. Caballero, R. Martínez-Sala, C. Rubio, J. Sánchez-Dehesa, F. Meseguer, J. Llinares, and F. Galves, "Sound attenuation by a two-dimensional array of rigid cylinders," Phys. Rev. Lett. **80**, 5325–5228 (1998).
[10] C. Rubio, D. Caballero, J. Sánchez-Pérez, R. Martinez-Sala, J. Sánchez-Dehesa, F. Meseguer, and F. Cervera, "The existence of full gaps and deaf bands in two-dimensional sonic crystals," J. of Lightwave Technology **17**, 2202–2207 (1999).
[11] D. Caballero, J. Sanchez-Dehesa, C. Rubio, R. Martinez-Sala, J. V. Sanchez-Perez, F. Meseguer, and J. Llinares, "Large two-dimensional sonic band gaps," Phys. Rev. E **60**, R6316–R6319 (1999).
[12] L. Sanchis, F. Cervera, J. Sánchez-Dehesa, J. V. Sánchez-Pérez, C. Rubio, and R. Martínez-Sala, "Reflectance properties of two-dimensional sonic band-gap crystals," J. Acoust. Soc. Am. **109**, 2598 (2001).
[13] I. E. Psarobas, N. Stefanou, and A. Modinos, "Scattering of elastic waves by periodic arrays of spherical bodies," Phys. Rev. B **62**, 278–291 (2000).
[14] I. E. Psarobas, N. Stefanou, and A. Modinos, "Phononic crystals with planar defects," Phys. Rev. B **62**, 5536–5540 (2000).
[15] I. E. Psarobas, A. Modinos, R. Sainidou, and N. Stefanou, "Acoustic properties of colloidal crystals," Phys. Rev. B **65**, 064307 (2002).
[16] F.-L. Hsiao, A. Khelif, H. Moubchir, A. Choujaa, C.-C. Chen, and V. Laude, "Complete band gaps and deaf bands of triangular and honeycomb water-steel phononic crystals," J. Appl. Phys. **101**, 044903 (2007).
[17] J.-H. Sun and T.-T. Wu, "Propagation of acoustic waves in phononic-crystal plates and waveguides using a finite-difference time-domain method," Phys. Rev. B **76**, 104304 (2007).
[18] T.-C. Wu, T.-T. Wu, and J.-C. Hsu, "Waveguiding and frequency selection of lamb waves in a plate with a periodic stubbed surface," Phys. Rev. B **79**, 104306 (2009).
[19] M. Gorisse, S. Benchabane, G. Teissier, C. Billard, A. Reinhardt, V. Laude, E. Defaÿ, and M. Aïd, "Observation of band gaps in the gigahertz range and deaf bands in a hypersonic aluminum nitride phononic crystal slab," Appl. Phys. Lett. **98**, 234103 (2011).
[20] D. Royer and E. Dieulesaint, *Elastic waves in solids* (Wiley, New York, 1999).
[21] R. J. P. Engelen, D. Mori, T. Baba, and L. Kuipers, "Subwavelength structure of the evanescent field of an optical bloch wave," Phys. Rev. Lett. **102**, 023902 (2009).
[22] M. I. Hussein, "Reduced bloch mode expansion for periodic media band structure calculations," Proceedings of the Royal Society A-Mathematical Physical and Engineering Sciences **465**, 2825–2848 (2009).